

¹ **The Morphological Diversification of Siphonophore Tentilla**

³ Alejandro Damian-Serrano^{1,‡}, Steven H.D. Haddock², Casey W. Dunn¹

⁴ ¹ Yale University, Department of Ecology and Evolutionary Biology, 165 Prospect St.,
⁵ New Haven, CT 06520, USA

⁶ ² Monterey Bay Aquarium Research Institute, 7700 Sandholdt Rd., Moss Landing, CA
⁷ 95039, USA

⁸ [‡] Corresponding author: Alejandro Damian-Serrano, email: alejandro.damianserrano@
⁹ yale.edu

¹⁰ **Keywords**

¹¹ Siphonophora, tentilla, nematocysts, character evolution

₁₂ **Abstract**

₁₃ Siphonophores are free-living predatory colonial hydrozoan cnidarians found in every ocean
₁₄ of the world. Siphonophore tentilla (tentacle side branches) are unique biological structures
₁₅ for prey capture, composed of a complex arrangement of cnidocytes (stinging cells) bearing
₁₆ different types of nematocysts (stinging capsules) and auxiliary structures. Tentilla present
₁₇ an extensive morphological and functional diversity across species. While associations
₁₈ between tentilla form and diet have been reported, the evolutionary history giving rise to this
₁₉ morphological diversity is largely unexplored. Here we examine the evolutionary gains and
₂₀ losses of novel tentillum substructures and nematocyst types on the most recent siphonophore
₂₁ phylogeny. Tentilla have a precisely coordinated high-speed strike mechanism of synchronous
₂₂ unwinding and nematocysts discharge. Here we characterize the kinematic diversity of this
₂₃ prey capture reaction using high-speed video and find relationships with morphological
₂₄ characters. Since tentillum discharge occurs in synchrony across a broad morphological
₂₅ diversity, we evaluate how phenotypic integration is maintaining character correlations across
₂₆ evolutionary time. We found that the tentillum morphospace has low dimensionality, we
₂₇ identified instances of heterochrony and morphological convergence, and generated hypotheses
₂₈ on the diets of understudied siphonophore species. Our findings indicate that siphonophore
₂₉ tentilla are phenotypically integrated structures with a complex evolutionary history leading to
₃₀ a phylogenetically structured diversity of forms which are predictive of kinematic performance
₃₁ and feeding habits.

32 **Introduction**

33 Siphonophores have fascinated zoologists for centuries for their extremely subspecialized
34 colonial organization and integration. Today we have a comprehensive taxonomic coverage
35 on the morphological diversity of this group due to the extensive work of siphonophore
36 taxonomists in the past few decades (Pugh, 1983, 2001; Pugh & Harbison, 1986; Pugh &
37 Youngbluth, 1988; Hissmann, 2005; Haddock *et al.*, 2005; Dunn *et al.*, 2005; Bardi & Marques,
38 2007; Pugh & Haddock, 2010; Pugh & Baxter, 2014), which has been elegantly synthesized
39 in detailed synopses (Totton & Bargmann, 1965, @mapstone2014global). In addition, recent
40 advances in phylogenetic analyses of siphonophores (Munro *et al.*, 2018; Damian-Serrano *et al.*,
41 2019) have provided a macroevolutionary context to interpret this diversity. With these assets
42 in hand, we can now begin to study siphonophores from an orthogonal perspective, focusing
43 on the diversity and evolutionary history of specific structures. Here we focus on one of such
44 structures: the tentilla. Like many cnidarians, siphonophore tentacles bear side branches
45 (tentilla) with nematocysts (Fig. 1). But unlike other cnidarians, most siphonophore tentilla
46 are dynamic structures that react to prey encounters by rapidly unfolding the nematocyst
47 battery to slap around the prey. This maximizes the surface area of contact between the
48 nematocysts and the prey they fire upon. In addition, siphonophore tentilla present a
49 remarkable diversity of morphologies (Fig. 2), sizes, and nematocyst complements (Fig. 3).
50 Our overarching aim is to organize all this phenotypic diversity in a phylogenetic context,
51 and identify the evolutionary processes that generated it.

52 In (Damian-Serrano *et al.*, 2019), we collected the most extensive morphological dataset
53 on siphonophore tentilla and nematocysts using state-of-the-art microscopy techniques, and
54 expanded the taxon sampling of the phylogeny to disentangle the evolutionary history. The
55 analyses we carried out led to novel, generalizable insights into the evolution of pred-
56 atory specialization. The primary findings of that work were that generalists evolved from
57 crustacean-specialist ancestors, and that feeding specializations were associated with distinct
58 modes of evolution and character integration patterns. The work we present here is comple-

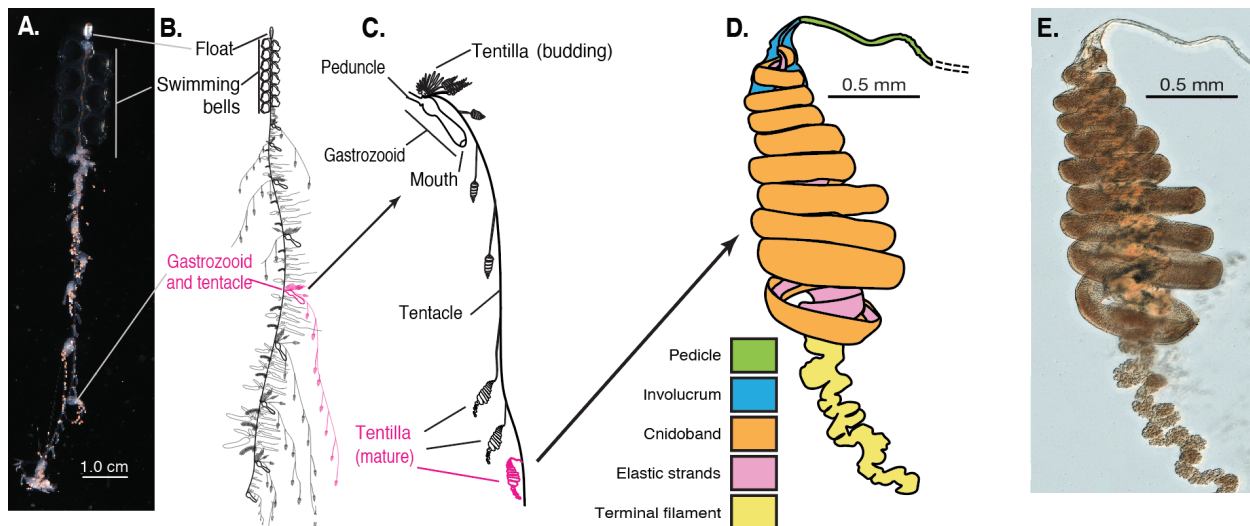


Figure 1: Siphonophore anatomy. A - *Nanomia* sp. siphonophore colony (photo by Catriona Munro). B, C - Illustration of a *Nanomia* colony, gastrozooid, and tentacle closeup (by Freya Goetz). D - *Nanomia* sp. Tentillum illustration and main parts. E - Differential interference contrast micrograph of the tentillum illustrated in D. Figure reproduced from Damian-Serrano et al. 2020 with permission. F. Action strip showing the behavior of tentilla during prey capture, illustrated by Riley Thompson.

59 mentary to (Damian-Serrano *et al.*, 2019), showcasing a far more detailed account on the
60 evolutionary history of tentilla morphology.

61 Nematocysts are unique biological weapons for defense and prey capture exclusive to the
62 phylum Cnidaria. Mariscal ((Mariscal, 1974)) reported that hydrozoans have the largest
63 diversity of nematocyst types among cnidarians. Among them, siphonophores present the
64 greatest variety of types (Mapstone, 2014), and vary widely across taxa in which and how
65 many types they carry on their tentacles (Fig. 3). Werner (Werner, 1965) noted that
66 there are nine types of nematocyst found in siphonophores, of which four, anacrophore
67 rhopalonemes, acrophore rhopalonemes, homotrichous anisorrhizas, and birhopaloids, are
68 unique to them. Heteroneme and haploneme nematocysts serve penetrant and entangling
69 functions, while rhopalonemes and desmonemes work by adhering to the surface of the prey.
70 While recent descriptive studies have expanded and confirmed our understanding of this
71 diversity, the evolutionary history of nematocyst type gain and loss in siphonophores remains
72 unexplored. Thus, here we reconstruct the evolution of shifts, gains, and losses of nematocyst

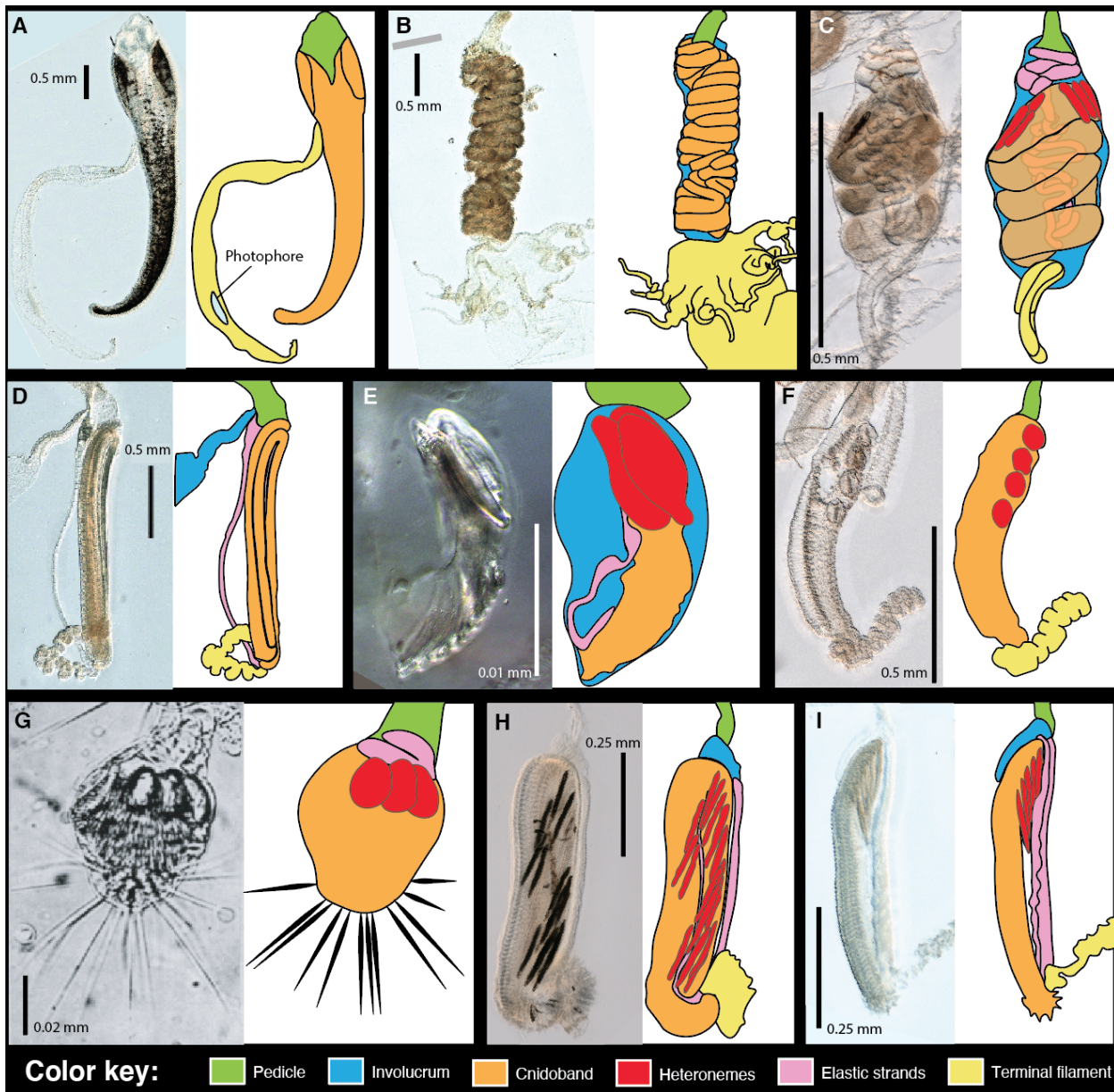


Figure 2: Tentillum diversity. The illustrations delineate the pedicle, involucrum, cnidoband, elastic strands, terminal structures. Heteroneme nematocysts (stenoteles in C,E,F,G and mastigophores in H,I) are only depicted for some species. A - *Erenna laciniiata*, 10x. B - *Lychnagalma utricularia*, 10x. C - *Agalma elegans*, 10x. D - *Resomia ornicephala*, 10x. E - *Frillagalma vityazi*, 20x. F - *Bargmannia amoena*, 10x. G - *Cordagalma* sp., reproduced from Carré 1968. H - *Lilyopsis fluoracantha*, 20x. I - *Abylopsis tetragona*, 20x.

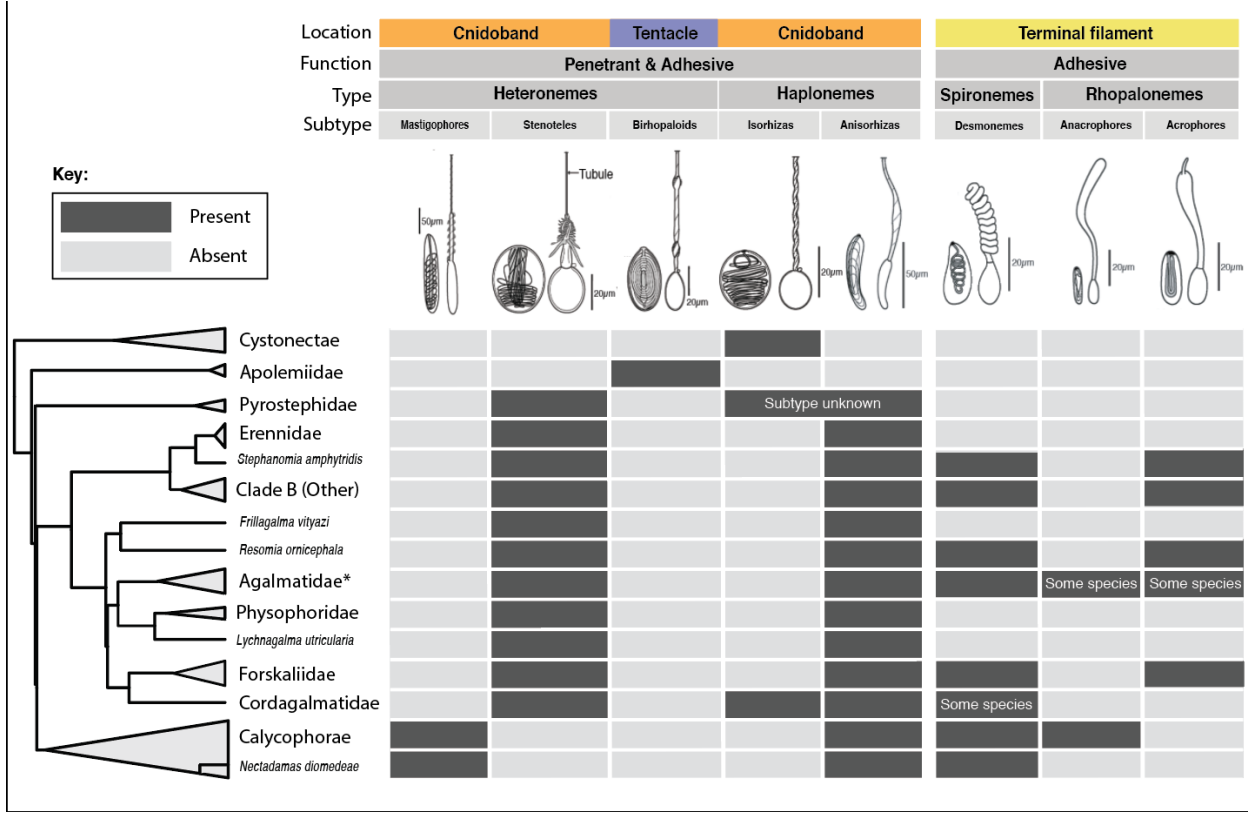


Figure 3: Phylogenetic distribution of nematocyst types, subtypes, functions, and locations in the zooid across the major siphonophore clades. Illustrations reproduced with permission from Mapstone (2014). Undischarged capsules to the left, discharged to the right. Agalmatidae* here refers only to the genera *Agalma*, *Athorybia*, *Halistemma*, and *Nanomia*.

73 types, subtypes, and other major categorical traits that led to the extant diversity we see in
 74 siphonophore tentilla.

75 Distantly related organisms that evolved to feed on similar resources often evolve similar
 76 adaptations (Winemiller *et al.*, 2015). In (Damian-Serrano *et al.*, 2019), we found strong
 77 associations between piscivory and haploneme shape across distantly related siphonophore
 78 lineages. These associations could have been produced by convergent changes in the adaptive
 79 optima of these characters. Here we set out to test this hypothesis using comparative
 80 model fitting methods. Analyzing the diversity of morphological states from a phylogenetic
 81 perspective allows us to identify the specific evolutionary processes that gave rise to it. Here
 82 we fit and compare a variety of macroevolutionary models to siphonophore tentilla morphology
 83 measurement data to identify instances of neutral divergence, stabilizing selection, changes in

84 the speed of evolution, and convergent evolution.

85 In (Damian-Serrano *et al.*, 2019) we fit discriminant analyses to identify characters that are
86 predictive of feeding guild. These discriminant analyses can be used to generate hypotheses
87 on the diets of ecologically understudied siphonophore species for which we have morphology
88 data. Here we present a Bayesian prediction for the feeding guild of 45 species uusing the
89 discriminant functions and morphological dataset in (Damian-Serrano *et al.*, 2019). As
90 mentioned above, tentilla are far from being ornamental shapes and are in fact violently
91 reactive weapons for prey capture (Mackie *et al.*, 1987; Damian-Serrano *et al.*, 2019). While
92 we now have detailed characterizations of tentilla morphologies across many species, the
93 diversity of dynamic performances and their relationships to the undischarged morphologies
94 have not been examined to date. To address this gap, we set out to record high-speed video
95 of the *in vivo* discharge dynamics of several siphonophore species at sea, and compare the
96 kinematic attributes to their morphological characters.

97 Methods

98 All character data and the phylogeny analyzed here were published in (Damian-Serrano
99 *et al.*, 2019). Details on the specimen collection, microscopy, and measurements can be
100 found in the aforementioned publication. However, we included here the character definitions
101 (SM14) and specimen list (SM15) in the Supporting Information. We log transformed all
102 the continuous characters that did not pass Shapiro-Wilks normality tests, and used the
103 ultrametric constrained Bayesian time tree in all comparative analyses. Inapplicable characters
104 were recorded as NA states, and species with states that could not be measured due to
105 technical limitations were removed before the analyses. We used the feeding guild categories
106 detailed in (Damian-Serrano *et al.*, 2019) with one modification: including all *Forskalia* spp.
107 as generalists instead of as a single *Forskalia* species on the tree after a reinterpretation
108 of the data in (Purcell, 1981). In order to characterize the evolutionary history of tentilla
109 morphology, we fitted different models generating the observed data distribution given the

phylogeny for each continuous character using the function `fitContinuous` in the R package *geiger* (Harmon *et al.*, 2007). These models include a non-phylogenetic white-noise model (WN), a neutral divergence Brownian Motion model (BM), an early-burst decreasing rate model (EB), and an Ornstein-Uhlenbeck (OU) model with stabilizing selection around a fitted optimum trait value. In the same way as (Damian-Serrano *et al.*, 2019) we then ordered the models by increasing parametric complexity (WN, BM, EB, OU), and compared their corrected Akaike Information Criterion (AICc) scores (Sugiura, 1978). We used the lowest (best) score using a delta cutoff of 2 units to determine significance relative to the next simplest model (SM10). We calculated model adequacy scores using the R package *arbutus* (Pennell *et al.*, 2015) (SM11), and calculated phylogenetic signals in each of the measured characters using Blomberg's K (Blomberg *et al.*, 2003) (SM10). To reconstruct the ancestral character states of nematocyst types and other categorical traits, we used stochastic character mapping (SIMMAP) using the package *phytools* (Revell, 2012).

In order to examine the phenotypic integration in the tentillum, we explored the relational structure among continuous characters and among their evolutionary histories using principal component analysis (PCA) and phylogenetic PCA (Revell, 2012). Since the character dataset contains gaps due to missing data and inapplicable character states, we carried out these analyses on a subset of species and characters that allowed for the most complete dataset. This was done by removing the terminal filament characters (which are only shared by a small subset of species), and then removing species which had inapplicable states for the remaining characters (apolemiids and cystonects). In addition, we obtained the correlations between the phylogenetic independent contrasts (Felsenstein, 1985) using the package *rphylip* (Revell & Chamberlain, 2014) accounting for intraspecific variation. Using these contrasts, we identified multivariate correlational modules among characters. To test and quantify phenotypic integration between these multivariate modules, we used the phylogenetic phenotypic integration test in the package *geomorph* (Adams *et al.*, 2016).

When comparing the morphospaces of species in different feeding guilds, we carried out

¹³⁷ a PCA on the complete character dataset while transforming inapplicable states of absent
¹³⁸ characters to zeros (i.e. cnidoband length = 0 when no cnidoband is present) to account
¹³⁹ for similarity based on character presence/absence. Using these principal components, we
¹⁴⁰ examined the occupation of the morphospace across species in different feeding guilds using a
¹⁴¹ phylogenetic MANOVA with the package *geiger* (Harmon *et al.*, 2007) to assess the variation
¹⁴² explained, and a morphological disparity test with the package *geomorph* (Adams *et al.*, 2016)
¹⁴³ to assess differences in the extent occupied by each guild.

¹⁴⁴ In order to detect and evaluate instances of convergent evolution, we used the package
¹⁴⁵ SURFACE (Ingram & Mahler, 2013). This tool identifies OU regimes and their optima
¹⁴⁶ given a tree and character data, and then evaluates where the same regime has appeared
¹⁴⁷ independently in different lineages. We applied these analyses to the haploneme nematocyst
¹⁴⁸ length and width characters as well as to the most complete dataset without inapplicable
¹⁴⁹ character states.

¹⁵⁰ In order to generate hypotheses on the diets of siphonophores using tentilla morphology,
¹⁵¹ we used the discriminant analyses of principal components (DAPC) (Jombart *et al.*, 2010)
¹⁵² trained in (Damian-Serrano *et al.*, 2019). We predict the feeding guilds of species in the
¹⁵³ dataset for which there are no published feeding observations using their morphological data
¹⁵⁴ as inputs, and presenting the predictive output in the form of posterior probabilities for each
¹⁵⁵ guild category.

¹⁵⁶ In order to observe the discharge behavior of different tentilla, we recorded high speed
¹⁵⁷ footage (1000-3000 fps) of tentillum and nematocyst discharge by live siphonophore specimens
¹⁵⁸ (26 species) using a Phantom Miro 320S camera mounted on a stereoscopic microscope. We
¹⁵⁹ mechanically elicited tentillum and nematocyst discharge using a fine metallic pin. We used
¹⁶⁰ the Phantom PCC software to analyze the footage. For the 10 species recorded, we measured
¹⁶¹ total cnidoband discharge time (ms), heteroneme filament length (μm), and discharge speeds
¹⁶² (mm/s) for cnidoband, heteronemes, haplonemes, and heteroneme shafts when possible (data
¹⁶³ available in the Dryad repository).

¹⁶⁴ **Results**

¹⁶⁵ *Evolutionary history of tentillum morphology* – In (Damian-Serrano *et al.*, 2019), we produced
¹⁶⁶ the most speciose siphonophore molecular phylogeny to date, while incorporating the most
¹⁶⁷ recent findings in siphonophore deep node relationships. This phylogeny revealed for the first
¹⁶⁸ time that the genus *Erenna* is the sister to *Stephanomia amphytridis*. *Erenna* and *Stephanomia*
¹⁶⁹ bear the largest tentilla among all siphonophores, thus their monophyly indicates that there
¹⁷⁰ was a single evolutionary transition to giant tentilla. Siphonophore tentilla range in size
¹⁷¹ from ~30 µm in some *Cordagalma* specimens to 2-4 cm in *Erenna* species, and up to 8 cm
¹⁷² in *Stephanomia amphytridis* (Pugh & Baxter, 2014). Most siphonophore tentilla measure
¹⁷³ between 175 and 1007 µm (1st and 3rd quartiles), with a median of 373 µm. The extreme
¹⁷⁴ gain of tentillum size in this newly found clade may have important implications for access
¹⁷⁵ to large prey size classes such as adult deep-sea fishes.

¹⁷⁶ Siphonophore tentilla are defined as lateral, monostichous evaginations of the tentacle
¹⁷⁷ (including its gastrovascular lumen), armed with epidermal nematocysts (Totton & Bargmann,
¹⁷⁸ 1965). The buttons on *Physalia* tentacles were not traditionally regarded as tentilla, but (Bardi
¹⁷⁹ & Marques, 2007) and our observations (Munro *et al.*, 2018), confirm that the buttons contain
¹⁸⁰ evaginations of the gastrovascular lumen, thus satisfying all the criteria for the definition.
¹⁸¹ In this light, and given that most Cystonectae bear conspicuous tentilla, we conclude (in
¹⁸² agreement with (Munro *et al.*, 2018) and (Damian-Serrano *et al.*, 2019)) that tentilla were
¹⁸³ present in the most recent common ancestor of all siphonophores, and secondarily lost twice,
¹⁸⁴ once in *Apolemia* and again in *Bathyphysa conifera*. In order to gain a broad perspective on
¹⁸⁵ the evolutionary history of tentilla, we reconstructed the phylogenetic positions of the main
¹⁸⁶ categorical character shifts using stochastic character mapping (SM1-9) and summarized in
¹⁸⁷ (Fig. 4). Some of these characters include the gain and loss of nematocyst types.

¹⁸⁸ We assume that haploneme nematocysts are ancestrally present in siphonophore tentacles
¹⁸⁹ since they are present in the tentacles of many other hydrozoans (Mariscal, 1974). Haplonemes
¹⁹⁰ are toxin-bearing open-ended nematocysts characterized by the lack of a shaft preceding

the tubule. Two subtypes are found in siphonophores: the isorhizas of homogeneous tubule width, and the anisorhizas with a slight bulking of the tubule near the base. In Cystonectae, haplonemes diverged into spherical isorhizas of two size classes. There is one size of haplonemes in Codonophora, which consist of elongated anisorhizas. Haplonemes were likely lost in the tentacles of *Apolemia* but retained as spherical isorhizas in other *Apolemia* tissues (Siebert *et al.*, 2013). While heteronemes exist in other tissues of cystonects, they appear in the tentacles of codonophorans exclusively, as birhopaloids in *Apolemia*, stenoteles in eucladophoran physonects, and microbasic mastigophores in calycophorans. The four nematocyst types unique to siphonophores appear in two events in the phylogeny (Fig. 4): birhopaloids arose in the stem to *Apolemia*, while rhopalonemes (acrophore and anacrophore) and homotrichous anisorhizas arose in the stem to Tendiculophora.

Nematocyst type gain and loss is also associated with prey capture functions. For example, the loss of desmonemes and rhopalonemes in piscivorous *Erenna*, retaining solely the penetrant (and venom injecting) anisothizas and stenoteles (two size classes) is reminiscent of the two size classes of penetrant isorhizas in the fish-specialist cystonects. Moreover, with the gain of anisorhizas, desmonemes, and rhopalonemes, the Tendiculophora gained versatility in entangling and adhesive functions of the cnidoband and terminal filament, which may have allowed their feeding niches to diversify. Part of the effectiveness of calycophoran cnidobands at entangling crustaceans may be attributed to the subspecialization of their heteronemes. These shifted from the ancestral penetrating stenotele to the microbasic mastigophore (or eurytele in some species) with a long barmed shaft with many long spines. This heteroneme subtype could be better at interlocking with the setae of crustacean legs and antennae.

In those species that have a functional terminal filament, the desmonemes and rhopalonemes play a fundamental role in the first stages of adhesion of the prey. In many species, the tugs of the struggling prey on the terminal filament trigger the cnidoband discharge (Mackie *et al.*, 1987 and pers. obs.). The adhesive terminal filament has been lost several times in the Euphysonectae (*Frillagalma*, *Lychnagalma-Physophora*, *Erenna*,

218 and some species of *Cordagalma*). In these species, we hypothesize that a different trigger
219 mechanism is at play, possibly involving the prey actively biting or grasping the tentillum or
220 lure.

221 The clades defined in (Damian-Serrano *et al.*, 2019) are characterized by unique evolu-
222 tionary innovations in their tentilla. The clade Eucladophora (containing Pyrostephidae,
223 Euphysonectae, and Calycophorae) encompasses all of the extant Siphonophore species (178
224 of 186) except Cystonects and *Apolemia*. Innovations that arose along the stem of this group
225 include spatially segregated heteroneme and haploneme nematocysts, terminal filaments, and
226 elastic strands (Fig. 4). Pyrostephids evolved a unique bifurcation of the axial gastrovascular
227 canal of the tentillum known as the “saccus” (Totton & Bargmann, 1965). The stem to
228 the clade Tendiculophora (clade containing Euphysonectae and Calycophorae) subsequently
229 acquired further novelties such as the desmoneme and rhopaloneme (acrophore subtype
230 ancestral) nematocysts on the terminal filament (Fig. 4), which bears no other nematocyst
231 type. These are arranged in sets of 2 parallel rhopalonemes for each single desmoneme (Skaer,
232 1988, 1991). The involucrum is an expansion of the epidermal layer that can cover part or
233 all of the cnidoband (Fig. 2). This structure, together with differentiated larval tentilla,
234 appeared in the stem branch to Clade A physonects. Calycophorans evolved novelties such as
235 larger desmonemes at the distal end of the cnidoband, pleated pedicles with a “hood” (here
236 considered homologous to the involucrum) at the proximal end of the tentillum, anacrophore
237 rhopalonemes, and microbasic mastigophore-type heteronemes. While calycophorans have
238 diversified into most of the extant described siphonophore species (108 of 186), their tentilla
239 have not undergone any major categorical gains or losses since their most recent common
240 ancestor. Nonetheless, they have evolved a wide variation in nematocyst and cnidoband
241 sizes. Ancestrally (and retained in most prayomorphs and hippopodids), the calycophoran
242 tentillum is recurved where the proximal and distal ends of the cnidoband are close together.
243 Diphyomorph tentilla are slightly different in shape, with straighter cnidobands.

244 *Evolution of tentillum and nematocyst characters –* Most (74%) characters present a

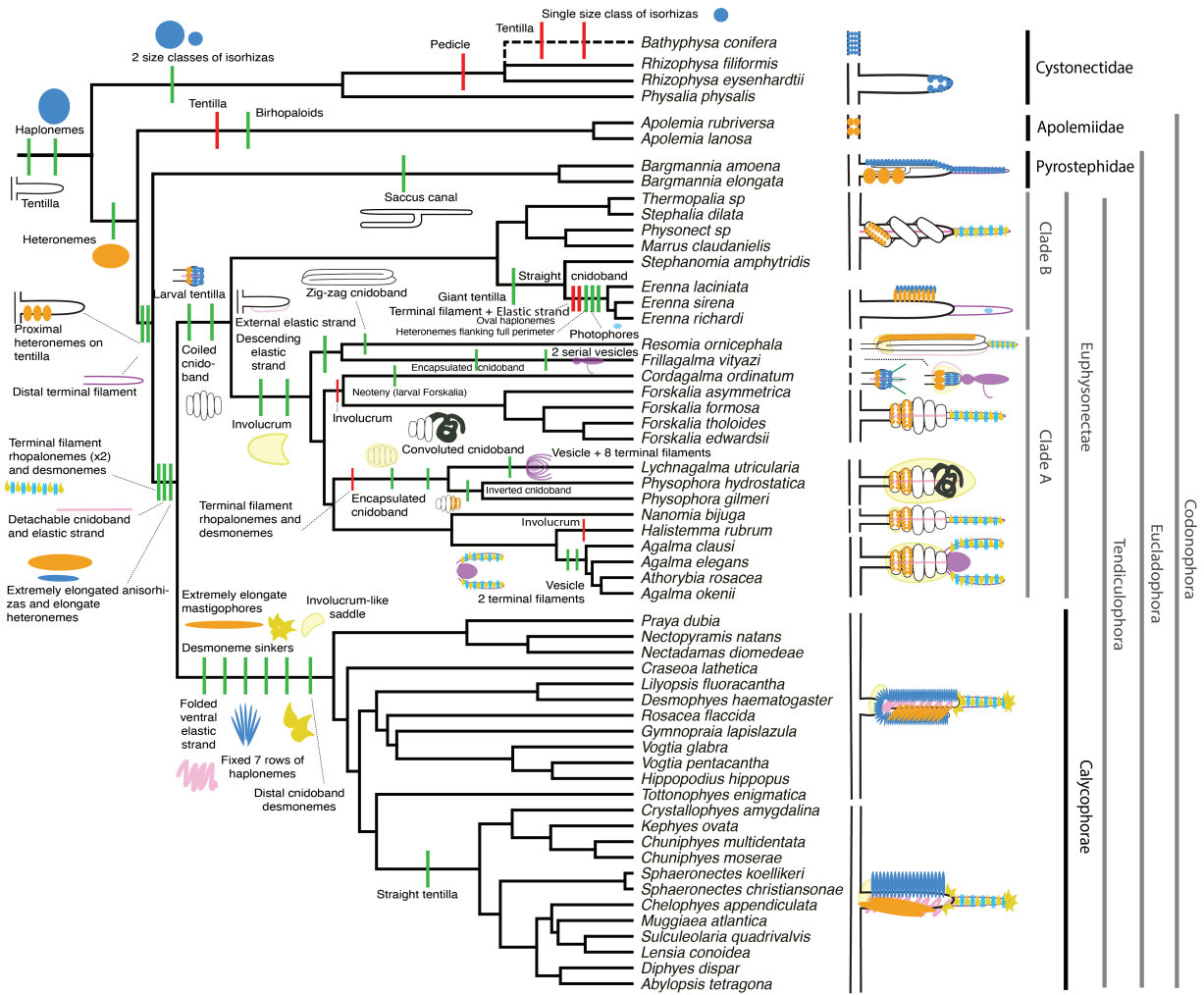


Figure 4: Siphonophore cladogram with the main categorical character gains (green) and losses (red) mapped. Some branch lengths were modified from the Bayesian chronogram to improve readability. The main visually distinguishable tentillum types are sketched next to the species that bear them, showing the location and arrangement of the main characters. In large, complex-shaped euphysonect tentilla, haplonemes were omitted for simplification. The hypothesized phylogenetic placement of the rhizophysid *Bathyphysa conifera*, for which no molecular data are yet available, was added manually (dashed line).

245 significant phylogenetic signal, yet only total nematocyst volume, haploneme length, and
246 heteroneme-to-cnidoband length ratio had a phylogenetic signal with K larger than 1. Total
247 nematocyst volume and cnidoband-to-heteroneme length ratio showed strongly conserved
248 phylogenetic signals. The majority (67%) of characters were best fitted by BM models,
249 indicating a history of neutral constant divergence. We did not find any relationship
250 between phylogenetic signal and specific model support, where characters with high and low
251 phylogenetic signal were broadly distributed among the best fitted for each model. One-third
252 of the characters measured in (Damian-Serrano *et al.*, 2019) did not recover significant support
253 for any of the phylogenetic models tested, indicating they are either not phylogenetically
254 conserved, or they evolved under a complex evolutionary process not represented among the
255 models tested (SM10). Haploneme nematocyst length was the only character with support
256 for an EB model of decreasing rate of evolution with time. No character had support for a
257 single-optimum OU model (when not informed by feeding guild regime priors). The model
258 adequacy tests (SM11) indicate that many characters may have a relationship between the
259 states and the rates of evolution (Sasr) not captured in the basic models compared here,
260 accompanied by a signal of unaccounted rate heterogeneity (Cvar). No characters show
261 significant deviations in the overall rate of evolution estimated (Msig). Some characters
262 show a perfect fit (no significant deviations across all metrics) under BM evolution, such as
263 heteroneme shape, length, width & volume, haploneme width & SA/V, tentacle width and
264 pedicle width. Haploneme row number and rhopaloneme shape have significant deviations
265 across four metrics, indicating that BM (best model) is a poor fit. These characters likely
266 evolved under complex models which would require many more data points than we have
267 available to fit with accuracy.

268 *Evolution of nematocyst shape* – The greatest evolutionary change in haploneme nema-
269 tocyst shape occurred in a single shift towards elongation in the stem of Tendiculophora,
270 which contains the majority of described siphonophore species, *i.e.* all siphonophores other
271 than Cystonects, *Apolemia*, and Pyrostephidae. There is one secondary return to more

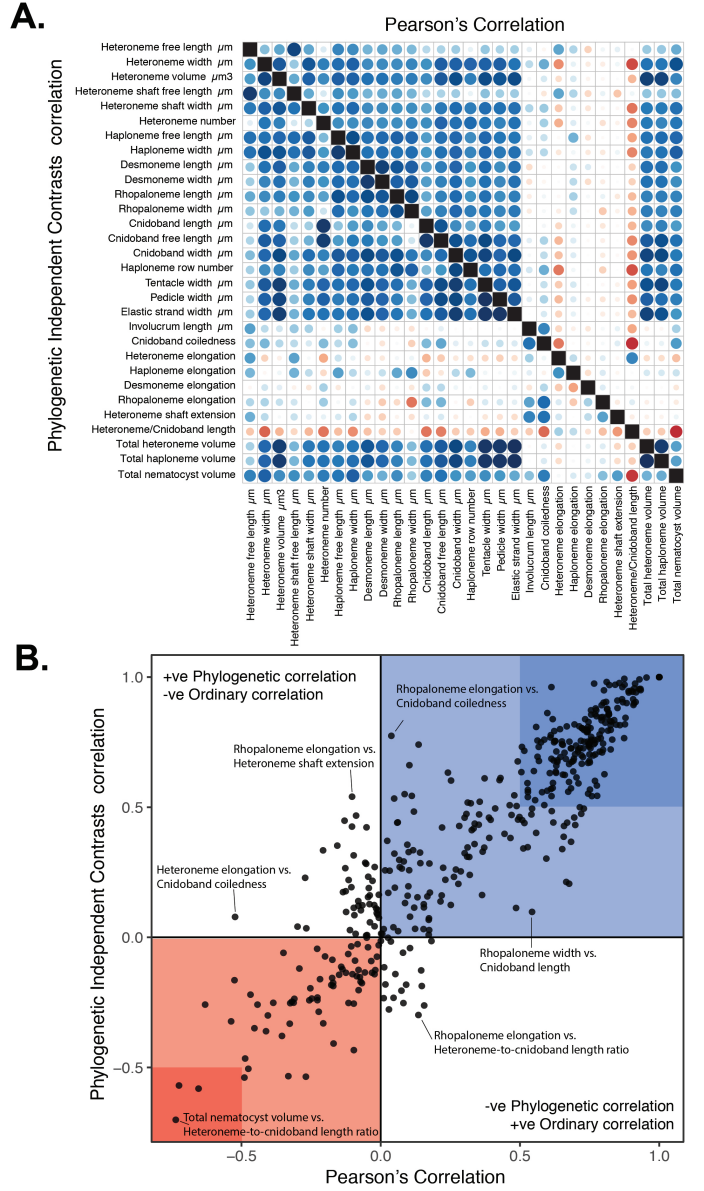


Figure 5: A. Correlogram showing strength of ordinary (upper triangle) and phylogenetic (lower triangle) correlations between characters. Both size and color of the circles indicate the strength of the correlation (R^2). B. Scatterplot of phylogenetic correlation against ordinary correlation showing a strong linear relationship ($R^2 = 0.92$, 95% confidence between 0.90 and 0.93). Light red and blue boxes indicate congruent negative and positive correlations respectively. Darker red and blue boxes indicate strong (<-0.5 or >0.5) negative and positive correlation coefficients respectively.

oval, less elongated haplonemes in *Erenna*, but it does not reach the sphericity present in Cystonectae or Pyrostephidae (Fig. 6). Heteroneme evolution presents a less discrete evolutionary history. Tendiculophora evolved more elongate heteronemes along the stem, but the difference between theirs and other siphonophores' is much smaller than the variation in shape within Tendiculophora, bearing no phylogenetic signal within this clade. In this clade, the evolution of heteroneme shape has diverged in both directions, and there is no correlation with haploneme shape (Fig. 6), which has remained fairly constant (elongation between 1.5 and 2.5).

Haploneme and heteroneme shape share 21% of their variance across extant values, and 53% of the variance in their shifts along the branches of the phylogeny. However, much of this correlation is due to the sharp contrast between Pyrostephidae and their sister group Tendiculophora. We searched for regime shifts in the evolution of haploneme nematocyst shape characters using SURFACE (Ingram & Mahler, 2013). SURFACE identified eight distinct OU regimes in the evolutionary history of haploneme length and width (Fig. 9A). The different regimes are located (1) in cystonects, (2) in most of Tendiculophora, (3) in most diphyomorphs, (4) in *Cordagalma ordinatum*, (5) in *Stephanomia amphytridis*, (6) in pyrostephids, (7) in *Diphyes dispar* + *Abylopsis tetragona*, and (8) in *Erenna* spp.

Phenotypic integration of the tentillum – Phenotypically integrated structures maintain evolutionary correlations between its constituent characters. Of the phylogenetic correlations (Fig. 5a, lower triangle), 81.3% were positive and 18.7% were negative, while of the ordinary correlations (Fig. 5a, upper triangle) 74.6% were positive and 25.4% were negative. Half (49.9%) of phylogenetic correlations were >0.5 , while only 3.6% are < -0.5 . Similarly, among the correlations across extant species, 49.1% were >0.5 and only 1.5% were < -0.5 . In addition, we found that 13.9% of character pairs had opposing phylogenetic and ordinary correlation coefficients. Just 4% have negative phylogenetic and positive ordinary correlations (such as rhopaloneme elongation ~ heteroneme-to-cnidoband length ratio and haploneme elongation, or haploneme elongation ~ heteroneme number), and only 9.9% of character pairs had positive

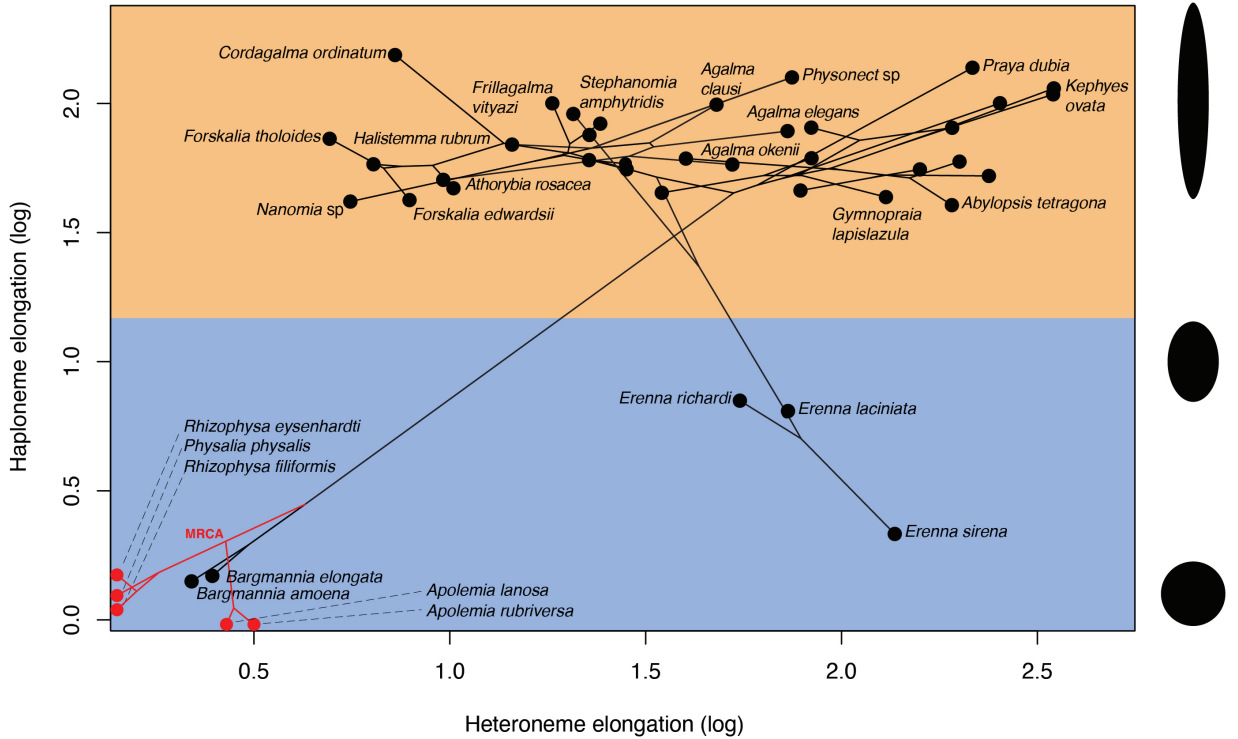


Figure 6: Phylomorphospace showing haploneme and heteroneme elongation (log scaled). Orange area delimits rod-shaped haplonemes, the blue area covers oval and round-shaped haplonemes. Smaller dots and lines represent phylogenetic relationships and ancestral states of internal nodes under BM. Species nodes in red lack either haplonemes or heteronemes, and their values are projected onto the axis of the nematocyst type they bear. Cystonects have no tentacle heteronemes and are projected onto the haploneme axis. Apolemiids have no tentacle haplonemes and are projected onto the heteroneme axis.

299 phylogenetic correlation yet negative ordinary correlation (such as heteroneme elongation ~
300 cnidoband convolution and involucrum length, or rhopaloneme elongation with cnidoband
301 length). These disparities could be explained by Simpson's paradox (Blyth, 1972): the
302 reversal of the sign of a relationship when a third variable (or a phylogenetic topology (Uyeda
303 *et al.*, 2018)) is considered. However, no character pair had correlation coefficient differences
304 larger than 0.64 between ordinary and phylogenetic correlations (heteroneme shaft extension
305 ~ rhopaloneme elongation has a Pearson's correlation of 0.10 and a phylogenetic correlation
306 of -0.54). Rhopaloneme elongation shows the most incongruencies between phylogenetic
307 and ordinary correlations with other characters. We identified four hypothetical modules
308 among the tentillum characters: (1) The tentillum scaffold module including cnidoband
309 length & width, nematocyst row number, pedicle & elastic strand width, tentacle width; (2)
310 the heteroneme module including heteroneme length & width, shafts length & width; (3)
311 the haploneme module including length and width; and (4) the terminal filament module
312 including desmoneme & rhopaloneme length & width. The phenotypic integration test showed
313 significant integration signal between all modules, tentillum and haploneme modules sharing
314 the greatest regression coefficient (SM12).

315 In the non-phylogenetic PCA morphospace using only characters derived from simple
316 measurements (Fig. 7), PC1 (aligned with tentillum and tentacle size) explained 69.3% of
317 the variation in the tentillum morphospace, whereas PC2 (aligned with heteroneme length,
318 heteroneme number, and haploneme arrangement) explained 13.5%. In a phylogenetic PCA,
319 63% of the evolutionary variation in the morphospace is explained by PC1 (aligned with
320 shifts in tentillum size), while 18% is explained by PC2 (aligned with shifts in heteroneme
321 number and involucrum length).

322 *Morphospace occupation* – In order to examine the occupation structure of the morphospace
323 across all siphonophore species in the dataset, we cast a PCA on the data after transforming
324 inapplicable states (due to absence of character) to zeroes. This allows us to accommodate
325 species with many missing characters (such as cystonects or apolemiids), and to account

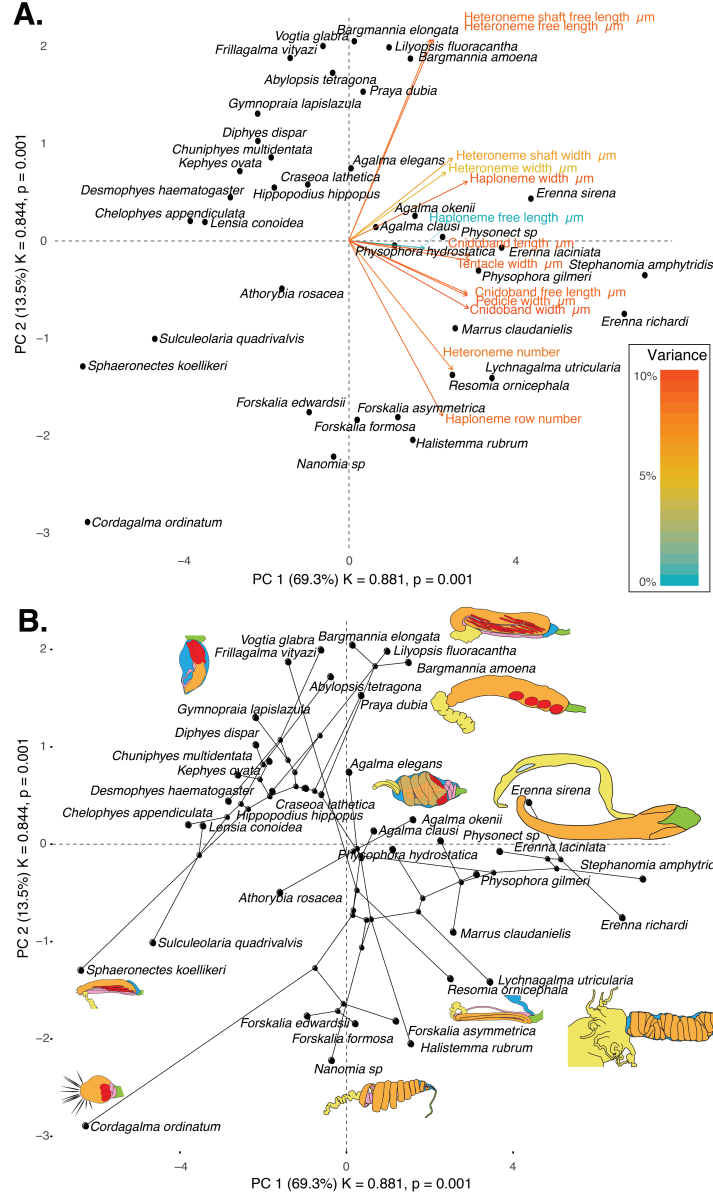


Figure 7: Phylomorphospace of the simple-measurement continuous characters principal components, excluding ratios and composite characters. A. Variance explained by each variable in the PC1-PC2 plane. Axis labels include the phylogenetic signal (K) for each component and p-value. B. Phylogenetic relationships between the species points and reconstructed ancestors distributed in that same space.

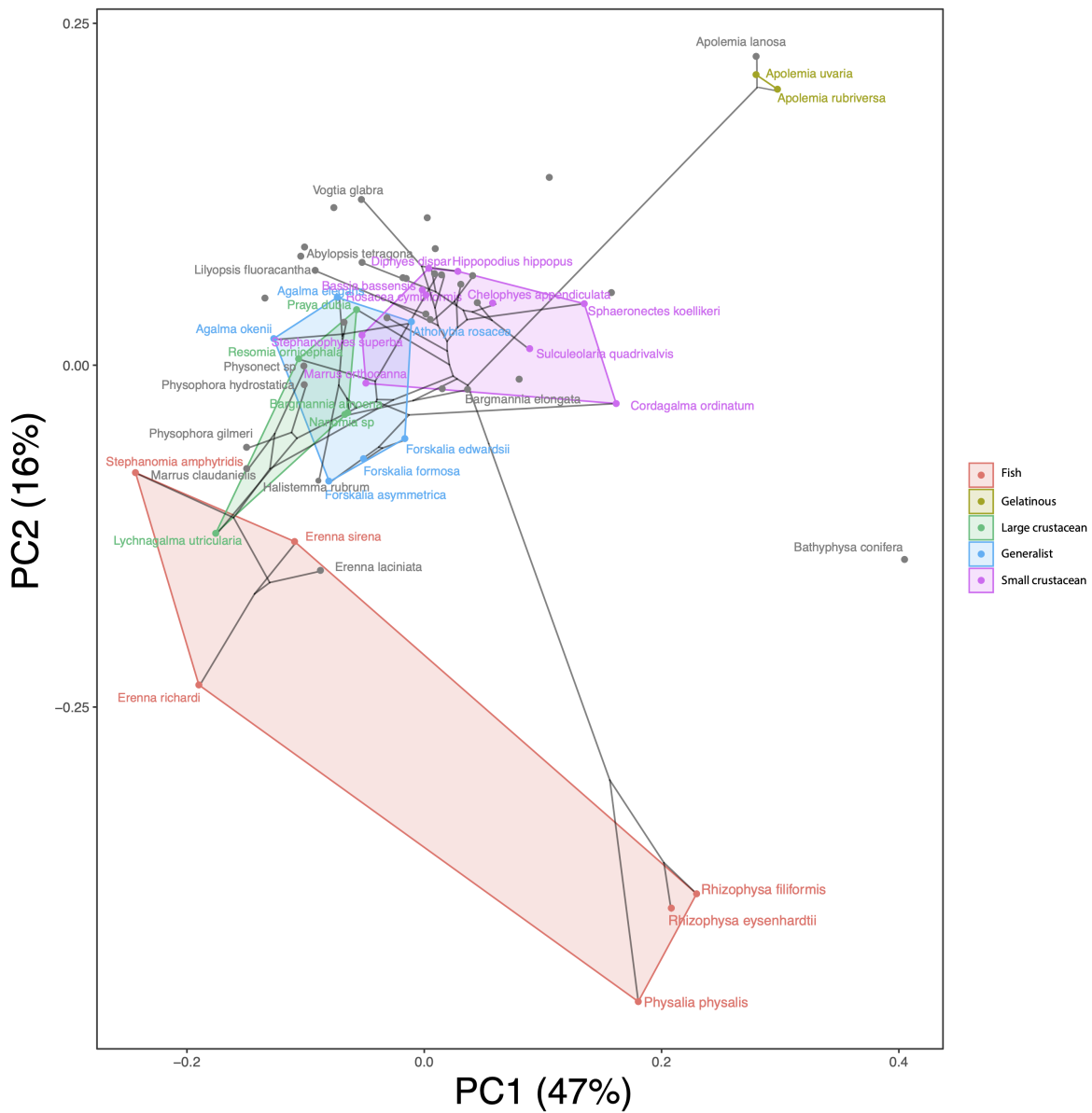


Figure 8: Phylomorphospace showing PC1 and PC2 from a PCA of continuous morphological characters with inapplicable states transformed to zeroes, overlapped with polygons conservatively defining the space occupied by each feeding guild. Lines between species coordinates show the phylogenetic relationships between them.

for common absences as morphological similarities. In this ordination, PC1 (aligned with cnidoband size) explains 47.45% of variation and PC2 (aligned with heteroneme volume and involucrum length) explains 16.73% of variation. When superimposing feeding guilds onto the morphospace (Fig. 8), we find that the morphospaces of each feeding guild are only slightly overlapping in PC1 and PC2. A phylogenetic MANOVA showed that feeding guilds explain 27.63% of variance across extant species (p value < 0.000001), and 20.97% of the variance when accounting for phylogeny, an outcome significantly distinct from the expectation under neutral evolution (p -value = 0.0196). In addition, a morphological disparity analysis accounting for phylogenetic structure shows that the morphospace of fish specialists is significantly broader than that of generalists and other specialists. This is due to the large morphological disparities between cystonects and piscivorous euphysonects. There are no significant differences among the morphospace disparities of the other feeding guilds.

Convergent evolution – Convergence is a widespread evolutionary phenomenon where distantly related clades independently evolve similar phenotypes. When the dimensionality of the state space is small as it is in tentilla morphology, convergence is more likely given the same amount of evolutionary change. Using the package SURFACE (Ingram & Mahler, 2013), we identified convergence in haploneme nematocyst shape and in morphospace position. In (Damian-Serrano *et al.*, 2019), we identified haploneme nematocyst shape as one of the traits associated with the convergent evolution of piscivory. Here we find that indeed wider haploneme nematocysts have convergently evolved in the piscivore cytonects and *Erenna* spp. (Fig. 9A). Extremely narrow haplonemes have also evolved convergently in *Cordagalma ordinatum* and copepod specialist calycophorans such as *Sphaeronectes koellikeri*. When integrating many traits into a couple principal components, we find two distinct convergences between euphysonects and calycophorans with a reduced prey capture apparatus. Those convergences are between *Frillagalma vityazi* and calycophorans, and once again between *Cordagalma ordinatum* and *Spaheronectes koellikeri* (Fig. 9B).

Functional morphology of tentillum and nematocyst discharge – Tentillum and nematocyst

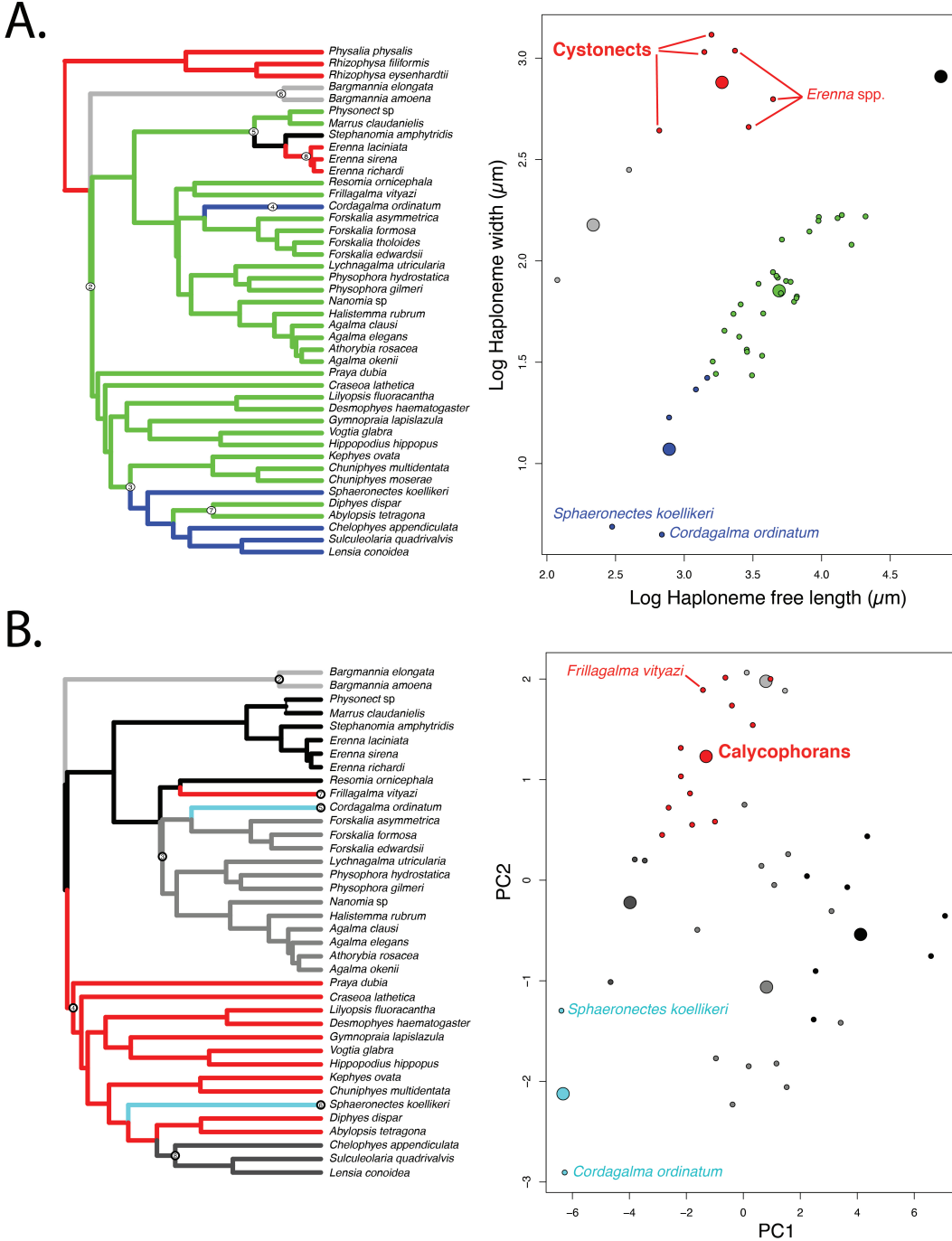


Figure 9: SURFACE plots showing convergent evolutionary regimes modelled under OU for (A) haploneme nematocyst length & width, and (B) for PC1 & 2 of all continuous characters with the exception of terminal filament nematocysts, and removing taxa with inapplicable character states. Node numbers on the tree label different regimes, regimes of the same color are identified as convergent. Small circles on the scatterplots indicate species values, large circles indicate the average position of the OU optima (θ) for a given combination of convergent regimes.

353 discharge high speed videos and measurements are available in the Dryad repository. While
354 the sample sizes of these measurements were insufficient to draw reliable statistical results
355 at a phylogenetic level, we did observe patterns that may be relevant to their functional
356 morphology. For example, cnidoband length is strongly correlated with discharge speed (p
357 value = 0.0002). This explains much of the considerable difference between euphysonect and
358 calycophoran tentilla discharge speeds (average discharge speeds: 225.0mm/s and 41.8mm/s
359 respectively; t-test p value = 0.011), since the euphysonects have larger tentilla than the
360 calycophorans among the species recorded. In addition, we observed that calycophoran
361 haploneme tubules fire faster than those of euphysonects (t-test p value = 0.001). Haploneme
362 nematocysts discharge 2.8x faster than heteroneme nematocysts (t-test p value = 0.0012).
363 Finally, we observed that the stenoteles of the Ephysonectae discharge a helical filament
364 that “drills” itself through the medium it penetrates as it everts.

365 *Generating dietary hypotheses using tentillum morphology* – For many siphonophore
366 species, no feeding observations have yet been published. To help bridge this gap of knowl-
367 edge, we generated hypotheses about the diets of these understudied siphonophores based
368 on their known tentacle morphology using one of the linear discriminant analyses of prin-
369 cipal components (DAPC) fitted in (Damian-Serrano *et al.*, 2019). This provides concrete
370 predictions to be tested in future work and helps extrapolate our findings to many poorly
371 known species that are extremely difficult to collect and observe. The discriminant analysis
372 for feeding guild (7 principal components, 4 discriminants) produced 100% discrimination,
373 and the highest loading contributions were found for the characters (ordered from highest
374 to lowest): Involutrum length, heteroneme volume, heteroneme number, total heteroneme
375 volume, tentacle width, heteroneme length, total nematocyst volume, and heteroneme width.
376 We used the predictions from this discriminant function to generate hypotheses about the
377 feeding guild of 45 species in the morphological dataset. This extrapolation predicts that
378 two other *Apolemia* species are gelatinous prey specialists like *Apolemia rubriversa*, and
379 predicts that *Erenna laciniata* is a fish specialist like *Erenna richardi*. When predicting soft-

³⁸⁰ and hard-bodied prey specialization, the DAPC achieved 90.9% discrimination success, only
³⁸¹ marginally confounding hard-bodied specialists with generalists (SM13). The main characters
³⁸² driving this discrimination are involucrum length, heteroneme number, heteroneme volume,
³⁸³ tentacle width, total nematocyst volume, total haploneme volume, elastic strand width, and
³⁸⁴ heteroneme length.

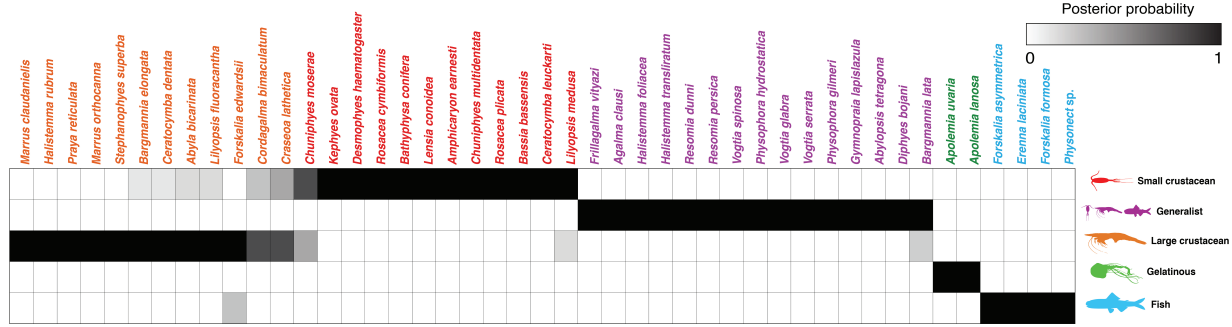


Figure 10: Hypothetical feeding guilds for siphonophore species predicted by a 6 PCA DAPC. Cell darkness indicates the posterior probability of belonging to each guild. The training dataset was transformed so inapplicable states are computed as zeroes. Species are sorted and colored according to their predicted feeding guild.

385 Discussion

386 *On the evolution of tentilla morphology* – The evolutionary history of siphonophore tentilla
 387 shows three major transition points which have structured the morphological diversity we
 388 see today. First, the earliest split between codonophorans and cystonects divides lineages
 389 with penetrating isorhizas from those which utilize heteronemes for prey capture. Second,
 390 the split between apolemiids and eucladophorans divided the simple-tentacled *Apolemia* from
 391 the lineage that evolved composite tentilla with heteronemes and haplonemes. Finally, the
 392 branch leading to tendiculophorans fostered innovations such as the elastic strands and the
 393 terminal filament nematocysts which produced the most complex tentilla structures and
 394 greatest morphological diversity we observe among siphonophores.

395 Siphonophore tentilla are beautifully complex and highly diverse. Our new analyses
 396 show, however, that the siphonophore tentillum morphospace actually has a fairly low extant
 397 dimensionality due to having an evolutionary history with many synchronous, correlated
 398 changes. This can be due to many causes including structural constraints, developmental
 399 constraints, or selection that reduces the viable state space. Though siphonophore development
 400 has not been extensively studied, what is known suggests that developmental constraints alone
 401 could not explain the highly correlated evolutionary changes we observe. The nematocysts
 402 that arm the tentillum are developed in a completely separate region of the gastrozooid

403 (Carré, 1972) and then migrate and assemble within the tentillum later on (Skaer, 1988).
404 This lack of proximity and physical independence of development between traits makes
405 developmental constraints unlikely. Surprisingly, many of the strong correlations we find
406 are between nematocyst and structural tentillum characters. Therefore, we hypothesize the
407 genetic correlations and phenotypic integration between tentillum and nematocyst characters
408 are maintained through natural selection on separate regulatory networks, out of the necessity
409 to work together and meet the spatial, mechanical, and functional constraints of their prey
410 capture behavior. In order to adequately test these hypotheses, future work would need to
411 study the genetic mechanisms underlying the development of tentilla from a comparative,
412 evolutionary approach. Fortunately, the unique biology of siphonophore tentacles displays
413 the full developmental sequence of tentilla along each tentacle, making siphonophores an
414 ideal system for the comparative study of development.

415 In (Damian-Serrano *et al.*, 2019) we examined the covariance terms in the multivariate rate
416 matrix for the evolution of tentillum and nematocyst characters. Building on this work, here
417 we examine the correlations among the trait values while accounting for phylogenetic structure.
418 The results for both analyses indicate that tentilla are not only phenotypically integrated (with
419 widespread evolutionary correlations across structures) but also show patterns of evolutionary
420 modularity, where different sets of characters appear to evolve in stronger correlations among
421 each other than with other characters (Wagner, 1996). This may be indicative of the
422 underlying genetic and developmental dependencies among closely homologous nematocyst
423 types (such as desmonemes and rhopalonemes) and structures. In addition, these evolutionary
424 modules point to hypothetical functional modules. For example, the coiling degree of the
425 cnidoband and the extent of the involucrum have correlated rates of evolution, while the
426 involucrum may help direct the whiplash of the uncoiling cnidoband distally (towards the
427 prey). The evolutionary innovation of the Tendiculophora tentilla with shooting cnidobands
428 and modular regions may have facilitated further dietary diversification. A specific instance
429 of this may have been the access to the abundant small crustacean prey such as copepods.

430 The rapid darting escape response of copepods may preclude their capture in siphonophores
431 without shooting cnidobands. Dietary diversification may be related to the far greater number
432 of species in Tendicilophora than its relatives Cystonectae, Apolemiidae, and Pyrostephidae.

433 *Heterochrony and convergence in the evolution of tentilla with diet* - In addition to identi-
434 fying shifts in prey type, (Damian-Serrano *et al.*, 2019) revealed the specific morphological
435 changes in the prey capture apparatus associated with these changes. Copepod-specialized
436 diets have evolved independently in *Cordagalma* and some calycophorans. These evolutionary
437 transitions happened together with transitions to smaller tentilla with fewer and smaller
438 cnidoband nematocysts. We found that these morphological transitions evolved convergently
439 in these taxa. Tentilla are expensive single-use structures (Mackie *et al.*, 1987), therefore we
440 would expect that specialization in small prey would beget reductions in the size of the prey
441 capture apparatus to the minimum required for the ecological performance. Such a reduction
442 in size would require extremely fast rates of trait evolution in an ordinary scenario. However,
443 *Cordagalma*'s tentilla strongly resemble the larval tentilla (only found in the first-budded
444 feeding body of the colony) of their sister genus *Forskalia*. This indicates that the evolution of
445 *Cordagalma* tentilla could be a case of paedomorphic heterochrony associated with predatory
446 specialization on smaller prey. This developmental shift may have provided a shortcut for
447 the evolution of a smaller prey capture apparatus.

448 Our work identifies yet another novel example of convergent evolution. The region of the
449 tentillum morphospace (Fig. 7 & Fig. 9B) occupied by calycophorans was independently (and
450 more recently) occupied by the physonect *Frillagalma vityazi*. Like calycophorans, *Frillagalma*
451 tentilla have small C-shaped cnidobands with a few rows of anisorhizas. Unlike calycophorans,
452 they lack paired elongate microbasic mastigophores. Instead, they bear exactly three oval
453 stenoteles, and their cnidobands are followed by a branched vesicle, unique to this genus.
454 Their tentillum morphology is very different from that of other related physonects, which tend
455 to have long, coiled, cnidobands with many paired oval stenoteles. Our SURFACE analysis
456 clearly indicates a regime convergence in the cnidoband morphospace between *Frillagalma* and

457 calycophorans (Fig. 9B). Most studies on calycophoran diets have reported their prey to be
458 primarily composed of small crustaceans, such as copepods or ostracods (Purcell, 1981, 1984).
459 The diet of *Frillagalma vityazi* is unknown, but this morphological convergence suggests that
460 they evolved to capture similar kinds of prey. The DAPCs in (Damian-Serrano *et al.*, 2019)
461 predict that *Frillagalma* has a generalist niche with both soft and hard-bodied prey, including
462 copepods.

463 *Evolution of nematocyst shape* – A remarkable feature of siphonophore haplonemes is
464 that they are outliers to all other Medusozoa in their surface area to volume relationships,
465 deviating significantly from sphericity (Thomason, 1988). This suggests a different mechanism
466 for their discharge that could be more reliant on capsule tension than on osmotic potentials
467 (Carré & Carré, 1980), and strong selection for efficient nematocyst packing in the cnidoband
468 (Thomason, 1988; Skaer, 1988). Our results show that Codonophora underwent a shift
469 towards elongation and Cystonectae towards sphericity, assuming the common ancestor had
470 an intermediate state. Since we know that the haplonemes of other hydrozoan outgroups are
471 generally spheroid, it is more parsimonious to assume that cystonects are simply retaining
472 this ancestral state. Later, we observe a return to more rounded (ancestral) haplonemes in
473 *Erenna*, concurrent with a secondary gain of a piscivorous trophic niche, like that exhibited by
474 cystonects. Our SURFACE analysis shows that this transition to roundness is convergent with
475 the regime occupied by cystonects (Fig. 9A). Purcell (Purcell, 1984) showed that haplonemes
476 have a penetrating function as isorhizas in cystonects and an adhesive function as anisorhizas
477 in Tendiculophora. It is no coincidence that the two clades that have converged to feed
478 primarily on fish have also converged morphologically toward more compact haplonemes.
479 Isorhizas in cystonects are known to penetrate the skin of fish during prey capture, and to
480 deliver the toxins that aid in paralysis and digestion (Hessinger, 1988). *Erenna*'s anisorhizas
481 are also able to penetrate human skin and deliver a painful sting (Pugh, 2001) (and pers.
482 obs.), a common feature of piscivorous cnidarians like the Portuguese man-o-war or box
483 jellies.

484 The implications of these results for the evolution of nematocyst function are that an
485 innovation in the discharge mechanism of haplonemes may have occurred during the main shift
486 to elongation. Elongate nematocysts can be tightly packed into cnidobands. We hypothesize
487 this may be a Tendiculophora lineage-specific adaptation to packing more nematocysts into
488 a limited tentillum space, as suggested by (Skaer, 1988). Thomason (Thomason, 1988)
489 hypothesized that smaller, more spherical nematocysts, with a lower surface area to volume
490 ratio, are more efficient in osmotic-driven discharge and thus have more power for skin
491 penetration. The elongated haplonemes of crustacean-eating Tendiculophora have never
492 been observed penetrating their crustacean prey (Purcell, 1984), and are hypothesized
493 to entangle the prey through adhesion of the abundant spines to the exoskeletal surfaces
494 and appendages. Entangling requires less acceleration and power during discharge than
495 penetration, as it does not rely on point pressure. In fish-eating cystonects and *Erenna* species,
496 the haplonemes are much less elongated and very effective at penetration, in congruence with
497 the osmotic discharge hypothesis. Tendiculophora, composed of the clades Euphysonectae
498 and Calycophorae, includes the majority of siphonophore species. Within these clades are the
499 most abundant siphonophore species, and a greater morphological and ecological diversity is
500 found. We hypothesize that this packing-efficient haploneme morphology may have also been
501 a key innovation leading to the diversification of this clade. However, other characters that
502 shifted concurrently in the stem of this clade could have been equally responsible for their
503 extant diversity.

504 *Generating hypotheses on siphonophore feeding ecology* – One motivation for our research
505 is to understand the links between prey-capture tools and diets so we can generate hypotheses
506 about the diets of predators based on morphological characteristics. Indeed, our discriminant
507 analyses were able to distinguish between different siphonophore diets based on morphological
508 characters alone. The models produced by these analyses generated testable predictions
509 about the diets of many species for which we only have morphological data of their tentacles.
510 For example, the unique tentilla morphology of *Frillagalma* is predicted to render a generalist

511 diet, or one of the undescribed deep-sea physonect species examined is predicted to be a
512 fish specialist, which if true would show a third instance of independently evolved piscivory.
513 While the limited dataset used here is informative for generating tentative hypotheses, the
514 empirical dietary data are still scarce and insufficient to cast robust predictions. This reveals
515 the need to extensively characterize siphonophore diets and feeding habits. In future work, we
516 will test these ecological hypotheses and validate these models by directly characterizing the
517 diets of some of those siphonophore species. Predicting diet using morphology is a powerful
518 tool to reconstruct food web topologies from community composition alone. In many of the
519 ecological models found in the literature, interactions among the oceanic zooplankton have
520 been treated as a black box (Mitra, 2009). The ability to predict such interactions, including
521 those of siphonophores and their prey, will enhance the taxonomic resolution of nutrient-flow
522 models constructed from plankton community composition data.

523 Acknowledgements

524 This work was supported by the Society of Systematic Biologists (Graduate Student Award
525 to A.D.S.); the Yale Institute of Biospheric Studies (Doctoral Pilot Grant to A.D.S.); and the
526 National Science Foundation (Waterman Award to C.W.D., NSF-OCE 1829835 to C.W.D.,
527 OCE-1829805 to S.H.D.H., and OCE-1829812 to C. Anela Choy). A.D.S. was supported by
528 a Fulbright Spain Graduate Studies Scholarship.

529 **References**

- 530 Adams, D.C., Collyer, M., Kaliontzopoulou, A., & Sherratt, E. (2016). Geomorph: Software
531 for geometric morphometric analyses.
- 532 Bardi, J. & Marques, A.C. (2007). Taxonomic redescription of the portuguese man-of-war,
533 physalia physalis (cnidaria, hydrozoa, siphonophorae, cystonectae) from brazil. *Iheringia.*
534 *Série Zoologia*, 97, 425–433.
- 535 Blomberg, S.P., Garland, T., & Ives, A.R. (2003). Testing for phylogenetic signal in
536 comparative data: Behavioral traits are more labile. *Evolution*, 57, 717–745.
- 537 Blyth, C.R. (1972). On simpson's paradox and the sure-thing principle. *Journal of the*
538 *American Statistical Association*, 67, 364–366.
- 539 Carré, D. (1972). Study on development of cnidocysts in gastrozooids of muggiaeae kochi
540 (will, 1844) (siphonophora, calycophora). *Comptes Rendus Hebdomadaires des Séances de*
541 *l'Academie des Sciences Serie D*, 275, 1263.
- 542 Carré, D. & Carré, C. (1980). On triggering and control of cnidocyst discharge. *Marine*
543 *& Freshwater Behaviour & Phy*, 7, 109–117.
- 544 Damian-Serrano, A., Haddock, S.H., & Dunn, C.W. (2019). The evolution of siphonophore
545 tentilla as specialized tools for prey capture. *bioRxiv*, 653345.
- 546 Dunn, C.W., Pugh, P.R., & Haddock, S.H. (2005). Marrus claudanielis, a new species of
547 deep-sea physonect siphonophore (siphonophora, physonectae). *Bulletin of Marine Science*,
548 76, 699–714.
- 549 Felsenstein, J. (1985). Phylogenies and the comparative method. *The American Naturalist*,
550 125, 1–15.
- 551 Haddock, S.H., Dunn, C.W., & Pugh, P.R. (2005). A re-examination of siphonophore
552 terminology and morphology, applied to the description of two new prayine species with
553 remarkable bio-optical properties. *Journal of the Marine Biological Association of the United*
554 *Kingdom*, 85, 695–707.
- 555 Harmon, L.J., Weir, J.T., Brock, C.D., Glor, R.E., & Challenger, W. (2007). GEIGER:

- 556 Investigating evolutionary radiations. *Bioinformatics*, 24, 129–131.
- 557 Hessinger, D.A. (1988). Nematocyst venoms and toxins. *The biology of nematocysts* (pp.
558 333–368). Elsevier.
- 559 Hissmann, K. (2005). In situ observations on benthic siphonophores (physonectae: Rho-
560 daliidae) and descriptions of three new species from indonesia and south africa. *Systematics
561 and Biodiversity*, 2, 223–249.
- 562 Ingram, T. & Mahler, D.L. (2013). SURFACE: Detecting convergent evolution from
563 comparative data by fitting ornstein-uhlenbeck models with stepwise akaike information
564 criterion. *Methods in ecology and evolution*, 4, 416–425.
- 565 Jombart, T., Devillard, S., & Balloux, F. (2010). Discriminant analysis of principal
566 components: A new method for the analysis of genetically structured populations. *BMC
567 genetics*, 11, 94.
- 568 Mackie, G.O., Pugh, P.R., & Purcell, J.E. (1987). Siphonophore Biology. *Advances in
569 Marine Biology*, 24, 97–262.
- 570 Mapstone, G.M. (2014). Global diversity and review of siphonophorae (cnidaria: Hydro-
571 zoa). *PLoS One*, 9, e87737.
- 572 Mariscal, R.N. (1974). Nematocysts.
- 573 Mitra, A. (2009). Are closure terms appropriate or necessary descriptors of zooplankton
574 loss in nutrient–phytoplankton–zooplankton type models? *Ecological Modelling*, 220, 611–620.
- 575 Munro, C., Siebert, S., Zapata, F., Howison, M., Serrano, A.D., Church, S.H., Goetz,
576 F.E., Pugh, P.R., Haddock, S.H., & Dunn, C.W. (2018). Improved phylogenetic resolution
577 within siphonophora (cnidaria) with implications for trait evolution. *Molecular Phylogenetics
578 and Evolution*,
- 579 Pennell, M.W., FitzJohn, R.G., Cornwell, W.K., & Harmon, L.J. (2015). Model adequacy
580 and the macroevolution of angiosperm functional traits. *The American Naturalist*, 186,
581 E33–E50.
- 582 Pugh, P. (1983). *Benthic siphonophores: A review of the family rhodaliidai (siphonophora,*

- 583 *physonectae*). Royal Society,
- 584 Pugh, P. (2001). A review of the genus erenna bedot, 1904 (siphonophora, physonectae).
- 585 *BULLETIN-NATURAL HISTORY MUSEUM ZOOLOGY SERIES*, 67, 169–182.
- 586 Pugh, P. & Baxter, E. (2014). A review of the physonect siphonophore genera halistemma
- 587 (family agalmatidae) and stephanomia (family stephanomiidae). *Zootaxa*, 3897, 1–111.
- 588 Pugh, P. & Haddock, S. (2010). Three new species of remosiid siphonophore (siphonophora:
- 589 Physonectae). *Journal of the Marine Biological Association of the United Kingdom*, 90, 1119–
- 590 1143.
- 591 Pugh, P. & Harbison, G. (1986). New observations on a rare physonect siphonophore,
- 592 lychnagalma utricularia (claus, 1879). *Journal of the Marine Biological Association of the*
- 593 *United Kingdom*, 66, 695–710.
- 594 Pugh, P. & Youngbluth, M. (1988). Two new species of prayine siphonophore (caly-
- 595 cophorae, prayidae) collected by the submersibles johnson-sea-link i and ii. *Journal of*
- 596 *Plankton Research*, 10, 637–657.
- 597 Purcell, J. (1981). Dietary composition and diel feeding patterns of epipelagic
- 598 siphonophores. *Marine Biology*, 65, 83–90.
- 599 Purcell, J.E. (1984). The functions of nematocysts in prey capture by epipelagic
- 600 siphonophores (coelenterata, hydrozoa). *The Biological Bulletin*, 166, 310–327.
- 601 Revell, L.J. (2012). Phytools: An r package for phylogenetic comparative biology (and
- 602 other things). *Methods in Ecology and Evolution*, 3, 217–223.
- 603 Revell, L.J. & Chamberlain, S.A. (2014). Rphylip: An r interface for phylip. *Methods in*
- 604 *Ecology and Evolution*, 5, 976–981.
- 605 Siebert, S., Pugh, P.R., Haddock, S.H., & Dunn, C.W. (2013). Re-evaluation of characters
- 606 in apolemiidae (siphonophora), with description of two new species from monterey bay,
- 607 california. *Zootaxa*, 3702, 201–232.
- 608 Skaer, R. (1988). *The formation of cnidocyte patterns in siphonophores*. Academic Press
- 609 New York,

- 610 Skaer, R. (1991). Remodelling during the development of nematocysts in a siphonophore.
611 216, 685–689.
- 612 Sugiura, N. (1978). Further analysts of the data by akaike's information criterion and the
613 finite corrections: Further analysts of the data by akaike's. *Communications in Statistics-*
614 *Theory and Methods*, 7, 13–26.
- 615 Thomason, J. (1988). The allometry of nematocysts. *The biology of nematocysts* (pp.
616 575–588). Elsevier.
- 617 Totton, A.K. & Bargmann, H.E. (1965). *A synopsis of the siphonophora*. British Museum
618 (Natural History),
- 619 Uyeda, J.C., Zenil-Ferguson, R., & Pennell, M.W. (2018). Rethinking phylogenetic
620 comparative methods. *Systematic Biology*, 67, 1091–1109.
- 621 Wagner, G.P. (1996). Homologues, natural kinds and the evolution of modularity. *Ameri-*
622 *can Zoologist*, 36, 36–43.
- 623 Werner, B. (1965). Die nesselkapseln der cnidaria, mit besonderer berücksichtigung der
624 hydriida. *Helgoländer wissenschaftliche Meeresuntersuchungen*, 12, 1.
- 625 Winemiller, K.O., Fitzgerald, D.B., Bower, L.M., & Pianka, E.R. (2015). Functional
626 traits, convergent evolution, and periodic tables of niches. *Ecology letters*, 18, 737–751.